DOI: 10.1002/ejoc.201000096

Tandem Photoarylation–Photoisomerization of Halothiazoles: Synthesis, Photophysical and Singlet Oxygen Activation Properties of Ethyl 2-Arylthiazole-5-carboxylates

Mario Amati,*[a] Sandra Belviso,[a] Maurizio D'Auria,[a] Francesco Lelj,[a] Rocco Racioppi,*[a] and Licia Viggiani[a]

Keywords: Heterocycles / Photochemistry / Arylation / Isomerization / Density functional calculations

The photochemical reaction between ethyl 2-chlorothiazole-5-carboxylate and benzene gave no product. In contrast, the reaction with ethyl 2-iodothiazole-5-carboxylate gave ethyl 3-phenylisothiazole-4-carboxylate. The same behaviour was observed if the reaction was performed in the presence of furan, thiophene and 2-bromothiophene. The products thus obtained were studied for their photophysical properties and it was found that the observed absorptions [λ_{max}=257 nm (ε = 7000 $M^{-1}\,cm^{-1}$) for ethyl 3-phenylisothiazole-4-carboxylate, 278 nm (ε = 7000 $M^{-1}\,cm^{-1}$) for ethyl 3-(2-furyl)isothiazole-4-carboxylate, 269 and 285 nm (ε = 7500 $M^{-1}\,cm^{-1}$) for ethyl 3-(2-thienyl)isothiazole-4-carboxylate] are mainly due to $\pi \rightarrow \pi^*$ transitions from the HOMO to the LUMO+1 orbital. The tested compounds showed fluorescence [λ_{em} = 350–400 (λ_{exc} = 300 nm), 360 and 410 nm (λ_{exc} = 320 nm), 412 nm (λ_{exc} = 340 nm) for ethyl 3-phenylisothiazole-4-carboxylate, 397 and 460 nm (λ_{exc} = 300 nm), 381, 394 and 460 nm (λ_{exc} = 320 nm), 381, 398 and 466 nm (λ_{exc} = 340 nm) for ethyl 3-(2-furyl)isothiazole-4-carboxylate, 372, 377 and 414 nm (λ_{exc} = 300, 320 and 340 nm respectively) for ethyl 3-(2-thienyl)isothiazole-4-carboxylate], possibly due to dual emission from different excited states. The use of the compound obtained as a sensitizer in the photo-oxidation of *trans*-α,α′-dimethylstilbene showed that all the new compounds are singlet-oxygen sensitizers.

Introduction

The photochemical reaction of halogen-substituted heterocyclic derivatives with aromatic and heteroaromatic compounds represents a useful synthetic methodology for obtaining the corresponding aryl and heteroaryl derivatives. We have found that a photochemical procedure can be used to obtain aryl-substituted furan, thiophene, pyrrole and imidazole derivatives bearing an electron-withdrawing group starting from the corresponding halogen-substituted compounds (Scheme 1).[1]

The reaction can be carried out with aldehydes or ketones in the starting material (**1a**–**d**, **1g**) as well with an ester function (**1e**). Substrates with more than one heteroatom (**1h**) can also be used in this type of reaction. The presence of a nitro group does not modify the behaviour when this substituent is present in a thiophene (**1f**) or in an imidazole ring (**1h**). Only in the presence of polyhalogenated thiophenes, such as **3**, did we observe a transposition of the halogen atom (Scheme 2). However, unusual behaviour was observed when 2-bromo-5-nitrothiazole (**6**) was used as the substrate (Scheme 2). In this case the photochemical reaction in the presence of aromatic compounds gave the corresponding 2-bromo-5-aryl derivatives with substitution of the nitro group.[2]

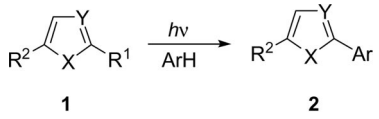

1 **2**

a: X = O, Y = CH, R^1 = Br, R^2 = COR
b: X = O, Y = CH, R^1 = I, R^2 = COR
c: X = S, Y = CH, R^1 = Br, R^2 = COR
d: X = S, Y = CH, R^1 = I, R^2 = COR
e: X = S, Y = CH, R^1 = I, R^2 = CO_2R
f: X = S, Y = CH, R^1 = I, R^2 = NO_2
g: X = NH, Y = CH, R^1 = I, R^2 = CHO
h: X = NH, Y = N, R^1 = I, R^2 = NO_2

Scheme 1. Photochemical reaction of halogen-substituted pentaatomic heterocycles with aromatic compounds.

Extension of the photoarylation reaction to the thiazole ring could provide interesting results from a synthetic viewpoint. In fact, Micrococcin P1, a member of the thiostrepton group of antibiotics, bears in the side-chain a thiazole linked to another thiazole through C-2 with a carboxamide moiety at C-4.[3]

[a] Dipartimento di Chimica, Università della Basilicata, Via N. Sauro 85, 85100 Potenza, Italy
Fax: +39-0971-202223
E-mail: mario.amati@unibas.it
rocco.racioppi@unibas.it

Supporting information for this article is available on the WWW under http://dx.doi.org/10.1002/ejoc.201000096.

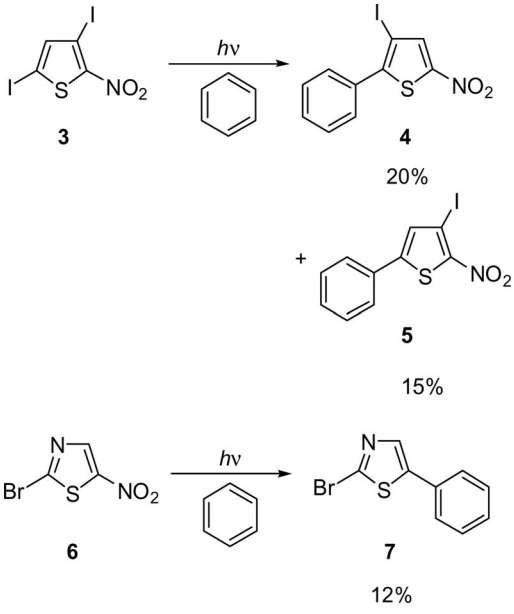

Scheme 2. Photochemical reactions of a polyhalogenated thiophene derivative and 2-bromo-5-nitrothiazole with benzene.

Hence, it would be interesting to verify if the above described reactivity is related to the specific nature of the nitro group, that is, its high electronegativity and deactivating character, or to the specificity of the heteroatomic ring. The ethyl 2-halothiazole-5-carboxylate (halogen: Cl and I) compounds allow the effect of varying the electronegativity and the presence of the deactivating ester moiety on the thiazole ring to be verified.

Furthermore, quantitative photophysics characterization and singlet-oxygen sensitizer properties of the coupling products are reported. In fact, in our previous work, it has been found that they can be used in the synthesis of natural and synthetic photobioactive compounds, the properties of which are related to their being singlet-oxygen sensitizers.[4]

Results and Discussion

We used ethyl 2-iodothiazole-5-carboxylate (**9**) as the starting material in this work. This compound was prepared as described previously from 2-trimethylsilylthiazole (**8**) (Scheme 3).[5] In that work ethyl 2-iodothiazole-5-carboxylate was obtained in 10% yield as the only reaction product. To obtain higher yields of the product, we performed the reaction in the presence of excess iodine. In this case **9** was obtained in higher yields (34%) together with a significant amount of ethyl 2-chlorothiazole-5-carboxylate (**10**; 18%). The higher yields could be attributed to the use of an excess of iodine instead of the stoichiometric amount used in the original work.

Under photochemical conditions, compound **9** readily reacted with benzene and other aromatic heterocyclic compounds. The irradiation of **9** in benzene gave a coupling product (Scheme 4, Table 1). The mass spectrum is in agreement with the formation of a product in which the iodine

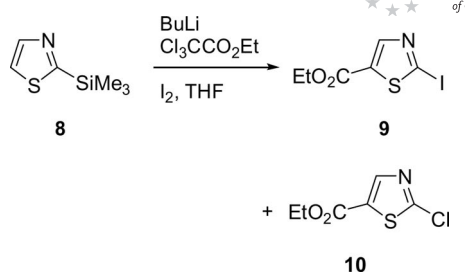

Scheme 3. Synthesis of ethyl 2-iodothiazole-5-carboxylate (**9**) and ethyl 2-chlorothiazole-5-carboxylate (**10**).

atom has been substituted with a phenyl group. However, the ^{1}H spectrum was not in agreement with the formation of ethyl 2-phenylthiazole-5-carboxylate.[6] On the contrary, the ^{1}H NMR spectrum is in agreement with that reported for ethyl 3-phenylisothiazole-4-carboxylate.[7] In particular, although the proton at C-4 in ethyl 2-phenylthiazole-5-carboxylate was expected at ca. 8.4 ppm,[6] we observed a signal at δ = 9.4 ppm, in agreement with that reported for ethyl 3-phenylisothiazole-4-carboxylate (δ = 9.32 ppm).[7] The ^{13}C NMR spectrum showed signals at δ = 168.9, 155.9 and 129.6 ppm, in agreement with those reported for the carbon atoms in the isothiazole ring in ethyl 3-(4-methoxyphenyl)-isothiazole-4-carboxylate (δ = 168.0, 155.5 and 128.8 ppm).[8] Conclusive identification of the reaction product was obtained by performing a long-range HETCOR experiment. Assuming a C-4–5-H coupling constant of 3.5 Hz,[9] we observed a coupling between the signal at δ = 9.4 ppm in the ^{1}H NMR spectrum (the proton at C-5) and the signal at δ 129.6 ppm in the ^{13}C NMR spectrum (C-4).

To confirm the isomerization reaction we prepared ethyl 2-phenylthiazole 5-carboxylate (**15**) through a Suzuki reaction between **9** and phenylboronic acid in the presence of [$Pd_2(dba)_3$] (Scheme 5).[10] The spectral data of our synthesized compound are in agreement with those reported in the literature.[6] The irradiation of **15** in acetonitrile gave **11** as the only product, unequivocally revealed by the analytical data (Scheme 5).

This behaviour was confirmed by using other aromatic compounds in the photochemical reaction: furan, thiophene and 2-bromothiophene. The irradiation of **9** in the presence of furan gave ethyl 3-(2-furyl)isothiazole-4-carboxylate (**12**; Scheme 4, Table 1). The same types of products, **13** and **14**, were obtained with thiophene and 2-bromothiophene, respectively (Scheme 4, Table 1).

Also in these cases we observed the formation of a photoisomerized product. This indicates that in the photochemical reaction of **9** not only the iodine atom is replaced by the aromatic moiety but an isomerization also occurs. Although there are several examples of photoisomerization of substituted thiazoles in the literature,[11–19] this is the first example of photoisomerization during an arylation reaction. The isomerization product is considered consistent with an internal cyclization–isomerization (ICI) mechanism.

The isomerization of penta-atomic heterocyclic compounds is one of the most important photochemical reactions of this type of compound.[20] Five mechanisms can be

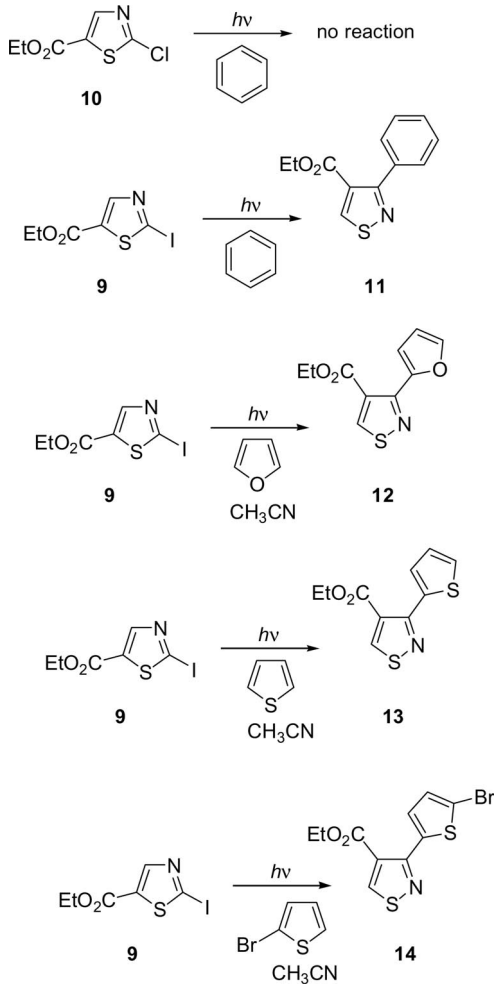

Scheme 4. Photochemical reactions of **9** and **10** with aromatic and heteroaromatic compounds.

Table 1. Photochemical arylation of ethyl 2-iodothiazole-5-carboxylate (**9**).

Substrate	Solvent	Aromatic compound	Irradiation time [h]	Product	Yield [%]
10	–	benzene	16	–	–
9	–	benzene	16	**11**	90
9	CH_3CN	furan	18	**12**	89
9	CH_3CN	thiophene	13.5	**13**	96[a]
9	CH_3CN	2-bromothiophene	34	**14**	35

[a] Compound **13** was obtained as a 10:1 mixture of 2-thienyl and 3-thienyl derivatives.

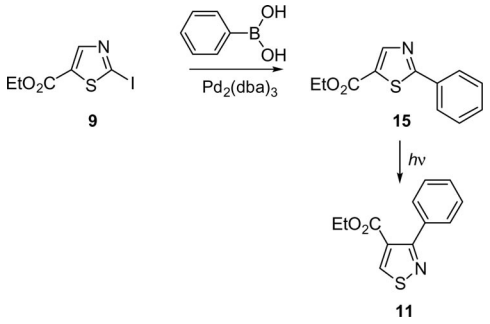

Scheme 5. Synthesis and photochemical isomerization of ethyl 2-phenylthiazole-5-carboxylate (**15**).

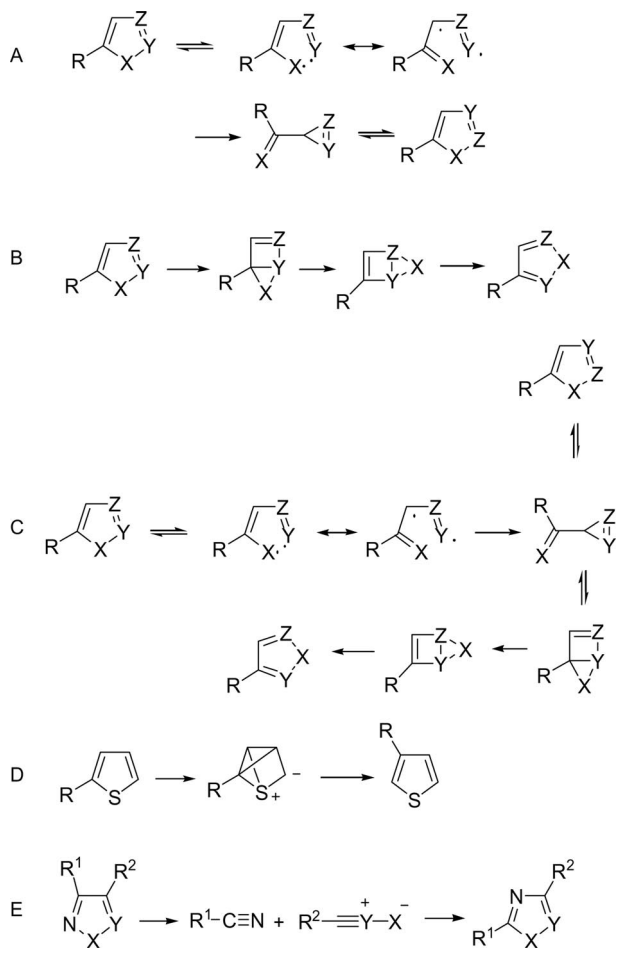

Scheme 6. Possible mechanisms for the photochemical isomerization of penta-atomic heterocyclic compounds.

invoked to justify the photochemical isomerization of penta-atomic aromatic heterocycles: i. ring contraction–ring expansion (RCRF; Scheme 6, A), ii. internal cyclization–isomerization (ICI; Scheme 6, B), iii. the van Tamelen–Whitesides general mechanism (VTW; Scheme 6, C), iv. the zwitterion–tricycle route (ZT; Scheme 6, D) and v. fragmentation–readdition (FR; Scheme 6, E).

Recently, we reported that the photochemical isomerization of penta-atomic aromatic heterocycles can be described by using a unifying hypothesis.[20] If the first excited singlet state of a molecule is populated, the molecule can convert into the corresponding triplet state or into the corresponding Dewar isomer. The efficiency of these processes will depend on energetic factors. If the Dewar isomer is formed, the isomeric product is obtained. If the triplet state is formed, cleavage of the X–C_α bond can occur to give ring-opened products, decomposition products or ring-contraction products. In this context, iodine favours intersystem crossing or the opening of the Dewar intermediate, as reported in Scheme 7.[14b]

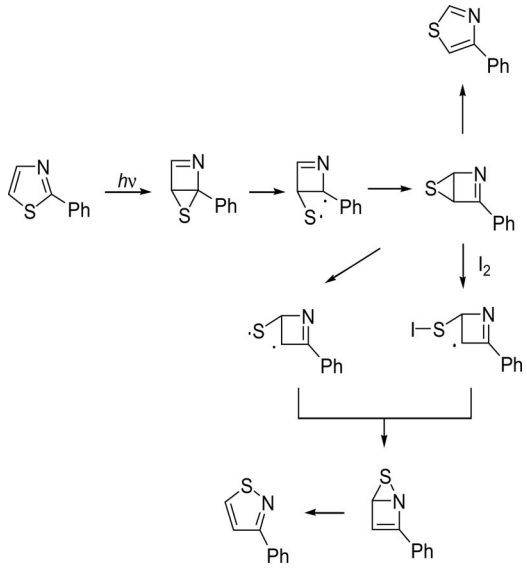

Scheme 7. Proposed mechanism for the photoisomerization of 2-phenylthiazole.

Compound **10** did not react when it was irradiated in benzene (Scheme 4); this lack of reactivity has already been observed in the case of 5-bromo-2-cyanothiophene.[1f]

These results, together with the previous results of reactions with nitro derivatives, strongly suggest that the reactivity of the thiazole ring is strongly affected by the nature of the substituent. In particular, the key step is the accessibility to the substituents at the C-2 position of low-energy σ radical species: both NO_2 and I substituents are more easily accessible and Cl, Br and CN or COOR groups are less accessible.

Furthermore, the presence of a phenyl ring at the 2-position can stabilize the diradical species thereby favouring the cleavage of the S–C bond of the Dewar intermediate on the excited-state energy surface.

It has been reported that some biaryl derivatives bearing electron-withdrawing groups can be used as singlet-oxygen sensitizers and show photodynamic activity.[4] To characterize the electronic structures of the investigated molecules a combined photophysical and computational study was carried out.[21]

Concerning the computational study, in the cases of **11**–**13** and **15**, the CO_2Et group was replaced by a CO_2Me group for computational convenience. Compound **11** showed two isomeric structures that differ in the orientation of the CO_2Me group. They are reported in Figure 1 and labelled as **11a** and **11b**. Structure **11a** is slightly more stable in energy (electronic energy in the Born–Oppenheimer approximation plus nuclei–nuclei electrostatic potential), differing by only 0.6 kcal/mol from **11b**. However, the computed spectroscopic properties of **11a** and **11b** are essentially equivalent such that only **11a** is discussed in the following paragraph. Similar results were found for **12**, **13** and **15**. The two orientations of the CO_2Me group are not relevant for the spectroscopic analyses and thus only one of the two isomers is discussed below. In **12** and **13**, the relative orientations of the furyl and thienyl groups give rise to a further two possible isomers for each compound (labelled with a and b in Figure 1). Compounds **12a** and **13a** are significantly more stable than **12b** and **13b** by 1.3 and 1.9 kcal/mol, respectively. Also in these cases, there are no large differences in the computed spectroscopic properties of the two isomers. Thus, only the most stable compounds **12a** and **13a** are the subject of the following discussion.

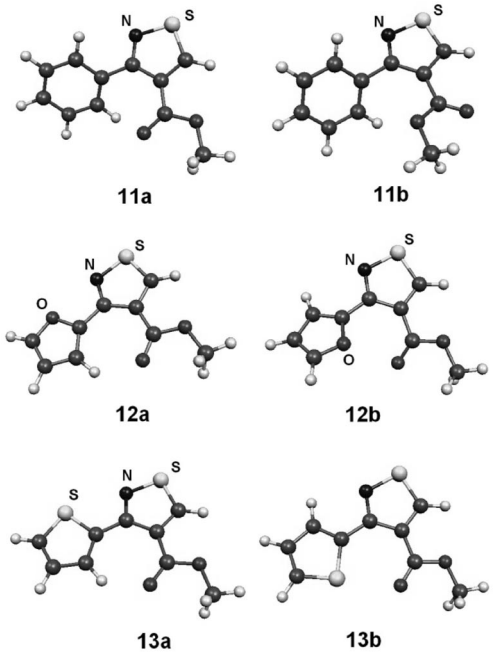

Figure 1. Some optimized structures for **11**–**13** determined at the B3LYP/6-31G(d,p) level of theroy.

The absorption spectra of **11**–**13** and **15** recorded in CH_3CN solution are reported in Figure 2 and the measured absorption values are collected in Table 2. To ensure that the photophysical properties measured were really due to the studied compounds and not to small impurities that could be present (especially in the case of fluorescence), the purity of **11**–**13** and **15** before and after the measurements was carefully checked by GC–MS analysis. As can be easily seen from the reported data, no impurities were detected (see the Supporting Information). Part a and b of Figure 2 show the experimental and computed absorption spectra of **15** and **11**, respectively. Both the experimental spectra show a single broad band with a maximum at 304 (**15**) and 257 nm (**11**). It is clear that the thiazole and isothiazole derivatives present different UV/Vis spectra and that the computations are able to reproduce such differences well.

According to the computations, excitation to the first excited state (S_1) of **15** is responsible for the absorption band at 304 nm. On the other hand, the band at 257 nm of **11** is assigned to transitions to S_3 and (mostly) S_4. In fact, S_1 and S_2 are described as weak transitions the presence of which explains the tail of the absorption spectrum at longer wavelengths that is absent in the experimental spectrum of **15**.

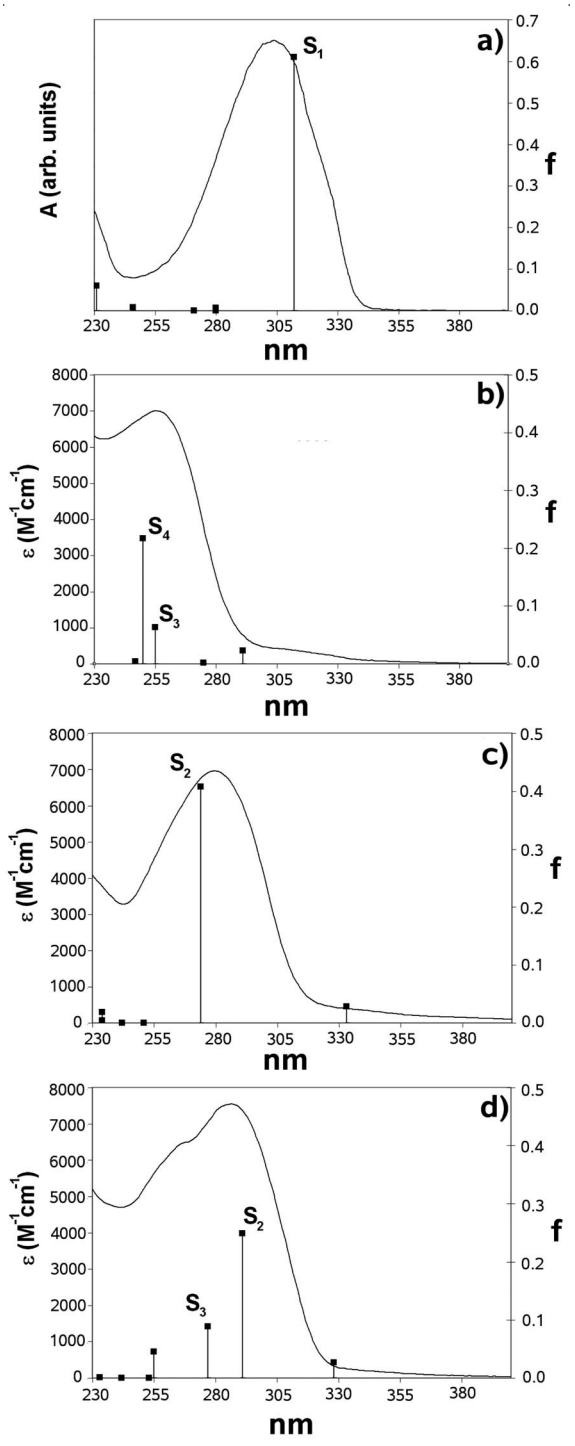

Figure 2. Experimental absorption spectra of (a) **15**, (b) **11**, (c) **12** and (d) **13** and, superimposed, the computed electronic vertical transitions of the structures **15**, **11a**, **12a** and **13a**.

Table 3 presents information about the low-energy excited states of the compounds studied and Figure 3 shows the Kohn–Sham orbital shapes useful for understanding the general characteristics of the excited states discussed. From Table 3 and Figure 3, the intense first band of **15** can be assigned to the $\pi \rightarrow \pi^*$ HOMO $\rightarrow$ LUMO (orbitals $57 \rightarrow 58$) transition. On the other hand, in the case of **11**, the first band is mainly assigned to the HOMO $\rightarrow$ (LUMO+1) (orbitals $57 \rightarrow 59$) monoelectronic excitation, which is the major component of S_4. From Figure 3 it is possible to note a certain similarity between the Kohn–Sham orbitals involved in the transitions. Orbital 58 in **15**, the LUMO, becomes orbital 59 in **11**, the LUMO+1, whereas orbital 57 is almost the same in both compounds. The UV/Vis absorptions S_1 and S_2 for **11** are $\pi \rightarrow \pi^*$ transitions assigned to the HOMO $\rightarrow$ LUMO (orbitals $57 \rightarrow 58$) and (HOMO-1) $\rightarrow$ LUMO (orbitals $56 \rightarrow 58$) monoelectronic excitations, respectively.

Table 2. Photophysical results obtained in CH_3CN solution for **11**–**13**.

	Absorption	Emission		
	λ_{abs} [nm] (ε [$M^{-1}cm^{-1}$])	λ_{em} [nm]	ϕ_F	τ[e] [ns]
11	257 (7000)	350–400[a] plateau 360 sh, 410[b] 412[c] 417[d]	0.018[a] 0.021[b] 0.10[c]	0.20 1.0[f]
12	278 (7000)	397, 460 sh[a] 381, 394, 460[b] 381, 398, 466[c] 466[d]	0.002[a] 0.022[b] 0.056[c]	2.0
13	269 sh, 285 (7500)	372[a] 377[b] 414[c] 484[d]	0.002[a] 0.005[b] 0.016[c]	0.5, 1.4[f]

[a] Excitation performed at 300 nm. [b] Excitation performed at 320 nm. [c] Excitation performed at 340 nm. [d] Excitation performed at 375 nm. [e] Lifetimes measured under excitation at 375 nm. [f] Dual exponential emission.

The assignment of transitions in the cases of **12** and **13** is similar to that of **11**. Also in this case, the HOMO→LUMO monoelectronic excitation is the main component of S_1, but the transition to S_1 is not assigned to the experimental absorption peaks at 278 (**12**) and 285 nm (**13**) (Figure 2 and Table 4). In both **12** and **13**, the intense absorption band is assigned to the transition to S_2, which is mainly due to the HOMO $\rightarrow$ (LUMO+1) monoelectronic excitation, as in **11**.

Note that according to the computations, the $n \rightarrow \pi^*$ excitations do not contribute to low-energy transitions. In the case of **11**, the first transition of this type is to S_5 computed at 248 nm. It involves a non-bonding occupied orbital localized on the CO_2Me carbonyl oxygen. The transition to S_6 at 230 nm is the first $n \rightarrow \pi^*$ transition that involves a non-bonding orbital of an aromatic heteroatom (the nitrogen non-bonding pair in the isothiazole ring).

The fact that $n \rightarrow \pi^*$ transitions are relatively high in energy is due to the higher electronegativity of the oxygen, nitrogen and sulfur atoms in comparison with carbon atoms. The occupied π orbitals are mainly localized on the less electronegative aromatic carbon atoms. Hence, they are closer in energy to π^* orbitals and lead to low-energy $\pi \rightarrow \pi^*$ transitions. Similar behaviour was observed for **12** and **13**.

Table 3. Computed UV/Vis transitions of **11**–**13** and **15**.

	Excited state	Energy [nm; eV]	Oscillator strength	Composition (%)	
15	S_1	312; 3.98	0.6097	57→58	81.09
11	S_1	291; 4.25	0.0230	57→58	88.67
				57→59	2.26
	S_2	275; 4.51	0.0020	54→58	2.01
				56→58	93.31
	S_3	255; 4.86	0.0629	54→58	16.02
				54→59	4.89
				56→59	37.34
				57→59	21.11
				57→60	4.74
				57→61	3.92
	S_4	250; 4.96	0.2168	54→58	5.05
				55→58	4.99
				56→59	14.50
				57→59	60.12
				57→61	4.16
12	S_1	333; 3.72	0.0282	54→55	90.18
				54→56	3.94
	S_2	274; 4.52	0.4080	54→55	2.15
				54→56	77.61
13	S_1	328; 3.78	0.0266	58→59	86.19
				58→60	7.41
	S_2	291; 4.26	0.2489	57→59	17.32
				58→59	3.97
				58→60	63.07
	S_3	277; 4.26	0.0887	57→59	80.73
				58→60	12.37

The emission spectra of compounds **11**–**13** in CH_3CN were recorded after excitation at λ_{ex} = 300, 320 and 340 nm, in the absorption tail range (Table 2 and Figure 4). The emission spectrum of the phenyl-substituted compound **11** obtained at λ_{ex} = 300 nm shows a very broad, plateau-like band in the 350–400 nm range, whereas at λ_{ex} = 320 and 340 nm a single, well-defined emission band is observed at around 410 nm. For compound **12**, a maximum at 397 nm was observed on excitation at λ_{ex} = 300 nm, whereas at λ_{ex} = 320 nm three distinct peaks with maxima at 381, 394 (the most intense) and 460 nm were observed. The same emission pattern is displayed on excitation at λ_{ex} = 340 nm with maxima at 381, 398 and 466 nm, the latter being the most intense. Similarly to the other compounds, the emission band of **13** evolves from a relatively weak band with a maximum at 372 nm to a more intense band with a maximum at 414 nm when λ_{ex} changes from 300 to 340 nm. For compounds **11**–**13** the quantum yields at each excitation wavelength were also measured by using anthracene in EtOH solution as a standard. As inferred from Table 2, the highest values are measured for λ_{ex} = 340 nm for the three compounds and, of these, the phenyl-substituted compound **11** seems to be the best emitter (quantum yield: 0.10 for λ_{ex} = 340 nm).

To understand the nature (fluorescence or phosphorescence) of the observed emission phenomena, lifetime measurements were also performed on the compounds **11**–**13**. The lifetimes were measured by using a 375 nm nanoLED and measuring the resulting emission intensity at the appropriate wavelength. The lifetimes were evaluated by an exponential fitting of the experimental data. As reported in

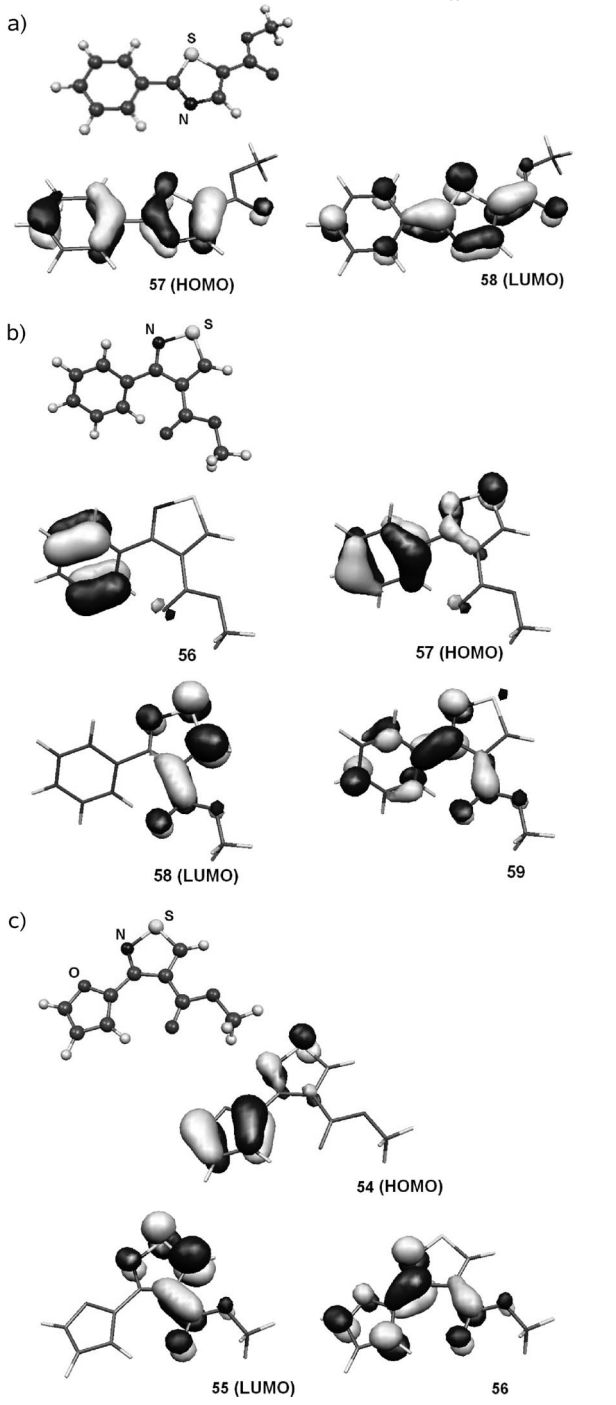

Figure 3. Some Kohn–Sham orbitals computed for (a) **15**, (b) **11** and (c) **12**. The orbitals of **13** are very similar to those of **12**, the only difference is that the HOMO is the 58th orbital and the LUMO is the 59th.

Table 4. Computed S_1 in its relaxed geometry (emission wavelengths).

	Energy [nm; eV]	Oscillator strength	Composition (%)	
11	347; 3.58	0.0157	57→58	97.1
12	400; 3.10	0.0210	54→55	98.3
13	401; 3.09	0.0175	58→59	98.1

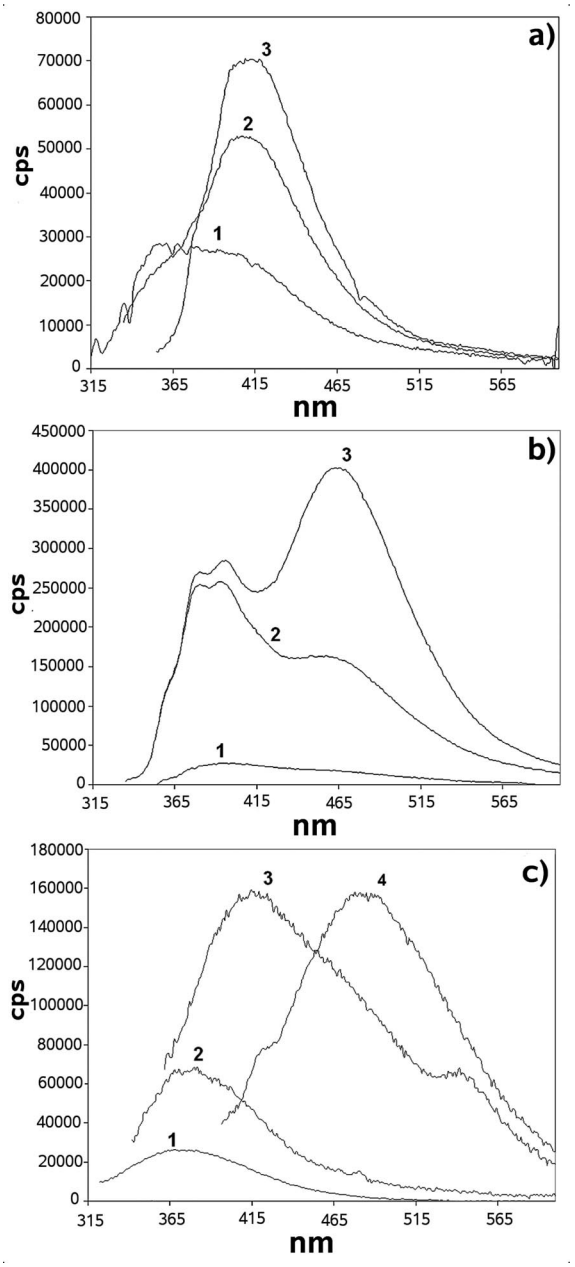

Figure 4. (a) Emission spectra of **11** recorded in CH_3CN with excitation wavelengths of (1) 300 nm and an absorbance of 0.0068, (2) 320 nm and an absorbance of 0.0207 and (3) 340 nm and an absorbance of 0.0010. (b) Emission spectra of **12** recorded in CH_3CN with excitation wavelengths of (1) 300 nm and an absorbance of 0.0238, (2) 320 nm and an absorbance of 0.0239 and (3) 340 nm and an absorbance of 0.0150. (c) Emission spectra of **13** recorded in CH_3CN with excitation wavelengths of (1) 300 nm and an absorbance of 0.0130, (2) 320 nm and an absorbance of 0.0171, (3) 340 nm and an absorbance of 0.0039 and (4) 375 nm reported in arbitrary units (cps: detector counts per seconds).

Table 2, the decay times were all in the range of 0.2–2.0 ns, which suggests that emission processes are a result of fluorescence.

As stated above, owing to the instrumental set-up, lifetimes were measured at an excitation wavelength (375 nm) higher than those used for recording the emission quantum yields. However, this does not influence the interpretation of the nature of the emissive phenomena. In fact, excitation at 375 nm of **11** and **12** gives rise to the same emission spectra described for λ_{ex} = 340 nm (Figure 4, a and b). Therefore lifetimes of the same magnitude (ns) have to be expected. In contrast, in **13**, for λ_{ex} = 375 nm, the observed emission band peak was redshifted by about 70 nm (Figure 4, c) and is similar to the emission band of **12** at λ_{ex} = 340 nm.

A computational analysis of the emission wavelengths of the compounds studied has also been achieved by optimizing the first and second singlet exited states of **11**–**13**. The study was focused only on the singlet excited states because lifetime measurements indicate that the emission process in solution at room temperature is due to fluorescence and not to phosphorescence. TD-DFT techniques were used as detailed in the Exptl. Sect. Some of the results are reported in Table 4. The computed emission peak wavelengths are not close to the experimental ones as in case of the absorption wavelength values. However, we note that very similar emission wavelengths are computed from S_1 in **12** and **13**. This fact could allow the assignment of the emission band of **12** at 466 nm and of **13** at 484 nm to S_1. If this is the case, an error of +0.45 and +0.42 eV is associated with the computation performed on **12** and **13**, respectively. In the case of **11**, emission from S_1 is computed to be at 347 nm. As in other compounds, it is blueshifted in comparison with the experimental S_1 emission peak that we place at 412 nm (Table 2). In this case the computation has an error of +0.58 eV.

If the above assignment is correct, the experimental emission bands at 350–360 nm for **11**, 381–398 nm for **12** and 372–414 nm for **13** (Table 2) should be assigned to emission from higher excited states. It is reasonable to assign such emissions to the S_2 excited state in the cases of **12** and **13** (Table 3 and Figure 2). In the case of **11**, S_3 and S_4 are additional possibilities to be taken into account. The fact that multiple decay times were recorded for **11** and **13** is a further indication of the presence of two emissive states.

Figure 5 shows the scaled excitation spectra of **13** recorded in CH_3CN solution. At the detection wavelength of 370 nm the excitation spectrum (spectrum 1 in Figure 5) is similar to the absorption spectrum. It is characterized by a peak wavelength of about 290 nm, which is very close to the absorption maximum at 285 nm (Table 2). At the detection wavelength of 470 nm (spectrum 3), the spectrum shows a broad emission in the excitation range of 290–370 nm. This spectrum should be associated with an emission process from a lower excited state. A comparison with spectrum 1 allows the absorption band of this excited state to be placed at wavelengths longer than 325 nm, in the long absorption tail of **13** (Figure 2).

According to our computations, the electronic transition to S_1 is localized at 328 nm (Table 3), in good agreement with experimental observations. Thus, spectrum 3 in Figure 5 is consistent with the presence of two concurrent phenomena: emission from S_1 after a barely effective internal conversion from a higher excited state and direct emission from S_1 after the $S_0 \rightarrow S_1$ transition. On the other hand,

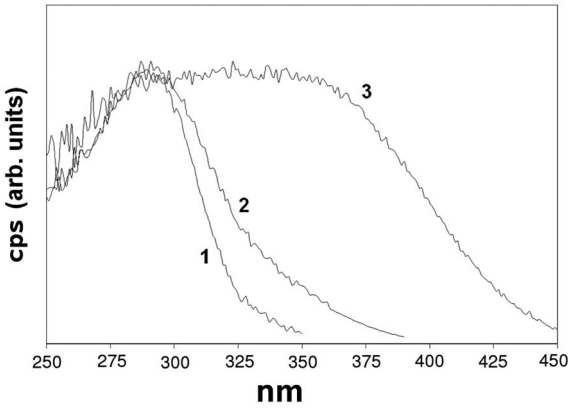

Figure 5. Scaled excitation spectra of **13** recorded in acetonitrile solution at detection wavelengths of (1) 370 nm, (2) 410 nm and (3) 470 nm. Spectrum 2 has been scaled by a factor 9.0 and spectrum 3 by a factor 34.5. Spectra 2 and 3 have been smoothed to reduce the amount of instrumental noise.

spectrum 1 is consistent with emission from a higher excited state (S_2 according to our computation) before internal conversion to S_1 and intersystem crossing to triplet states take place.

To add more support to this suggestion, it is important to analyse the composition of the singlet states in terms of monoelectronic transitions and their f_{0j} oscillator strengths. From Table 3 it can be seen that, in the case of **11**, S_3 and S_4 have a large contribution from the $56 \rightarrow 59$ and $57 \rightarrow 59$ monoelectronic excitations, whereas S_1 has only a very small contribution from the $57 \rightarrow 59$ (2.26%) monoelectronic excitation. Similar behaviour can be observed for **12** (S_2) and **13** (S_2 and S_3).

In a perturbative framework, the probability of transition from an excited state j to another state k is given by the relationship (1)[22] in which H_v is the vibronic operator describing the perturbation that couples the S_k and S_j states. They in turn are expressed as a linear combination of monoelectronic excitations within each Slater determinant (Table 3). In these terms, if the two excited states have very different compositions, the numerator of the previous equation is expected to be small enough to reduce the kinetic constant of the non-radiative decaying process from higher- to lower-energy excited states. This could prevent a fast non-radiative decay from the higher S_i to S_1 and, together with a large oscillator strength for the transition from S_i to S_0, might allow emission from excited states higher than S_1, in contrast to the "Kasha principle", which assumes a faster non-radiative decay to S_1 and then a possible radiative decay to S_0.

$$P_{k \rightarrow j} \propto \frac{\left| < S_k | \mathrm{Hv} | S_j > \right|^2}{\Delta E_{kj}} \quad (1)$$

Singlet-Oxygen Activation

Photodynamic activity is usually divided into two processes named Type I and Type II.[23] In Type I reactions a triplet sensitizer reacts with the substrate or solvent by hydrogen abstraction or electron transfer. In Type II reactions the triplet sensitizer reacts with oxygen to give, by energy transfer, singlet oxygen or, by electron transfer, the superoxide ion (Scheme 8). If a compound is a singlet-oxygen sensitizer, the efficiency of the process depends on the efficiency of excited triplet-state generation.

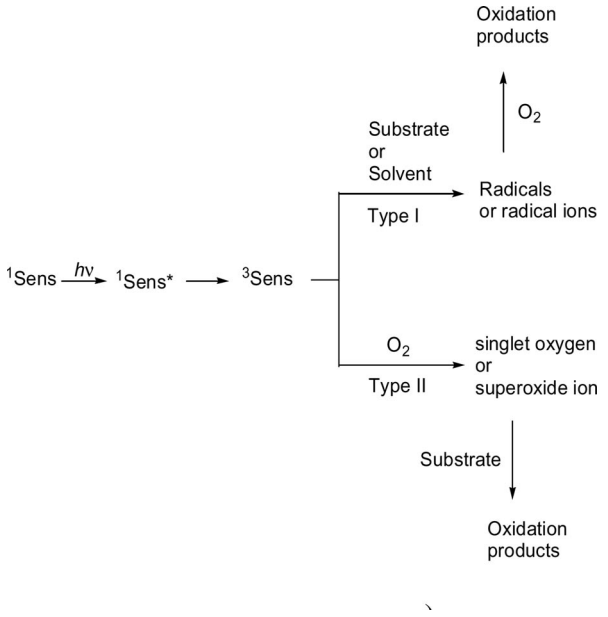

Scheme 8. Type I and Type II photodynamic activity.

It has been reported that irradiation of *trans*-α,α′-dimethylstilbene (**16**) in acetonitrile in the presence of both oxygen and a suitable sensitizer gives only compound **17** when the sensitizer produces singlet oxygen by a Type II reaction whereas if the sensitizer can undergo a Type I process, a completely different product mixture is obtained (Scheme 9).[24] This behaviour has been shown to be a useful method for distinguishing between Type I and Type II photosensitizers giving good results with both singlet oxygen[4f,4g,25] and electron-transfer sensitizers.[26]

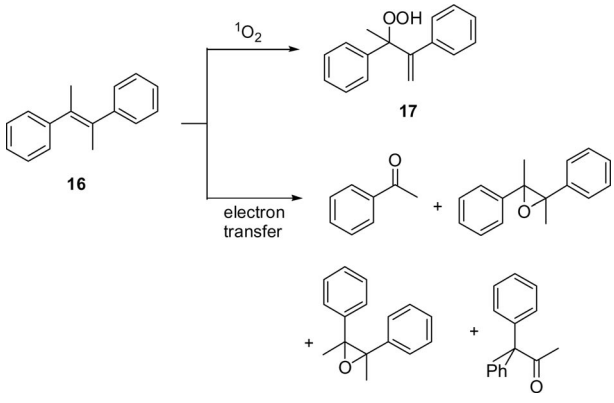

Scheme 9. Reactions of *trans*-α,α′-dimethylstilbene.

Furthermore, the absence of electron-transfer products in competition reactions[27] involving *trans*-α,α′-dimethylstilbene (**16**) indicates that it is an efficient $^1O_2$ acceptor

and a suitable substrate for studying singlet-oxygen sensitizers. Compounds **11**–**14** showed photosensitizer activity and in the photoreaction with **16** only the hydroperoxide **17** was obtained, which strongly suggests that they are able to generate singlet oxygen. Furthermore, a non-negligible quantum yield value of 0.07 ± 0.01 for singlet oxygen generation for the compound **11** was obtained by using α-terthiophene as actinometer ($\Phi_\Delta = 0.81$).[28]

Conclusions

The photochemical reactions between ethyl 5-iodothiazole-2-carboxylate and aromatic compounds gave the corresponding arylisothiazole derivatives in good yields. The reaction probably occurs by photoarylation and subsequent photoisomerization of the arylthiazole derivative. This is the first case of photoisomerization during a photoarylation reaction. The photophysical properties of the products thus obtained were studied and it was found that the observed absorptions are mainly due to $\pi \rightarrow \pi^*$ transitions from the HOMO to the LUMO+1 orbital. The compounds studied showed fluorescence in solution at room temperature. We have also shown that the low fluorescence quantum yields allow these compounds to be singlet-oxygen sensitizers and potentially useful compounds for photodynamic therapy.

Experimental Section

General: NMR spectra were recorded with a Bruker 300 AM or Varian Inova 500 instrument operating at 500 MHz. Mass spectra were obtained with a Hewlett–Packard 5890 gas chromatograph [OV-1 capillary column between 70 and 250 °C (20 °C/min)] with Hewlett–Packard 5971 mass-selective detector. UV spectra were recorded at room temperature in a double-ray UV/Vis/NIR 05E Cary Varian spectrophotometer in 1.0 cm optical path quartz cuvettes.

Unless otherwise indicated, photochemical reactions were performed in an immersion apparatus surrounded with a Pyrex water jacket with a 125 W high-pressure mercury arc (Helios-Italquartz, Milan, Italy).

Solvents used in physical measurements were spectroscopic or HPLC grade and obtained from Aldrich and Fluka.

Ethyl 2-Iodothiazole-5-carboxylate (9) and 2-Chlorothiazole-5-carboxylate (10): *n*BuLi (11.5 mL, 1.6 M in hexane) was added to a stirred solution of 2-trimethylsylilthiazole (**8**; 2.48 g, 16 mmol) in dry diethyl ether (50 mL) cooled to –78 °C. After 30 min, ethyl chloroformate (5.3 g, 48 mmol) was added and the resulting mixture stirred at –78 °C for a further 30 min and then at room temp. for 30 min. After recooling to –78 °C, excess I_2 in dry THF (50 mL) was added and the reaction slurry was slowly warmed to room temp. and stirred for 15 h, then recooled to –78 °C and treated with 20% sodium thiosulfate in water to destroy excess I_2. The mixture was then extracted three times with diethyl ether and the organic layers were washed with brine, dried with Na_2SO_4 and the solvents evaporated under vacuum to afford a crude mixture that was purified by chromatography over silica gel (eluent: 95:5 petroleum ether/ethyl acetate) to obtain 1.76 g of **9** (6.2 mmol, 34.2%) and 561 mg of **10** (2.0 mmol, 18.4%).

9: Oil. ^{1}H NMR (500 MHz, $CDCl_3$): δ = 1.32 (t, J = 7.1 Hz, 3 H, CH_3), 4.30 (q, J = 7.1 Hz, 2 H, CH_2), 8.04 (s, 1 H, 4-H) ppm. ^{13}C NMR (125 MHz, $CDCl_3$): δ = 14.4, 62.2, 108.2, 135.8, 149.4, 159.9 ppm. UV (CH_3CN): λ_{max} = 269 nm. MS: *m*/*z* (%) = 283 (63) $[M]^+$, 255 (100), 238 (86), 210 (24), 156 (11), 128 (6.6), 100 (8.2), 83 (22), 57 (12), 29 (9), 15 (0.3). $C_6H_6INO_2S$ (283.09): calcd. C 25.46, H 2.14, N 4.95, S 11.33; found C 25.53, H 2.05, N 5.01, S 11.25.

10: Oil. ^{1}H NMR (500 MHz, $CDCl_3$): δ = 1.28 (t, J = 7 Hz, 3 H, CH_3), 4.32 (q, J = 7 Hz, 2 H, CH_2), 8.10 (s, 1 H, 4-H) ppm. ^{13}C NMR (125 MHz, $CDCl_3$): δ = 14.4, 62.2, 131.7, 146.8, 157.2, 160.3 ppm. MS: *m*/*z* (%) = 191 (25) $[M]^+$, 193 (8.1) $[M + 2]^+$, 163 (73), 146 (100), 130 (7.1), 118 (82), 99 (11), 57 (36), 45 (17), 29 (30), 18 (3). $C_6H_6ClNO_2S$ (191.64): calcd. C 37.60, H 3.16, N 7.31, S 16.73; found C 37.52, H 3.08, N 7.39, S 17.80.

Ethyl 3-Phenylisothiazole-4-carboxylate (11): Compound **9** (736 mg, 2.6 mmol) was dissolved in anhydrous benzene (80 mL). The mixture was degassed with nitrogen for 1 h. The mixture was irradiated in an immersion apparatus with a 125 W high-pressure mercury arc and the reaction was monitored by TLC. After 16 h, the mixture was washed with 20% sodium thiosulfate in water to oxidize traces of iodine and then with brine, dried with Na_2SO_4 and the solvents evaporated under vacuum to afford a crude mixture that was purified by chromatography over silica gel (eluent: 98:2 to 96:4 petroleum ether/ethyl acetate) to give 545 mg (2.34 mmol, 90%) of **11** as an oil.

^{1}H NMR (500 MHz, $CDCl_3$): δ = 1.27 (t, J = 7.1 Hz, 3 H, CH_3), 4.28 (q, J = 7.1 Hz, 2 H, CH_2), 7.64–7.44 (m, 5 H, phenyl), 9.4 (s, 1 H, 5-H) ppm. ^{13}C NMR and DEPT (125 MHz, $CDCl_3$): δ = 14.3 (CH_3), 61.4 (CH_2), 128.1 (CH), 129.3 (CH), 129.4 (CH), 129.6 (C), 135.3 (C), 155.9 (CH), 162.3 (C), 168.9 (C) ppm. UV (CH_3CN): λ_{max} = 257 nm, ε = 7000 $dm^3 mol^{-1} cm^{-1}$. MS: *m*/*z* (%) = 233 (86.3) $[M]^+$, 204 (34.2), 188 (100), 161 (19.7), 116 (8.7), 85 (6.7), 77 (9), 57 (9.3), 29 (3.9). $C_{12}H_{11}NO_2S$ (233.29): calcd. C 61.78, H 4.75, N 6.00, S 13.74; found C 61.70, H 4.86, N 6.07, S 13.68.

Ethyl 3-(2-Furyl)isothiazole-4-carboxylate (12): Compound **9** (945 mg, 3.3 mmol) was added to furan (3 g) in acetonitrile (80 mL). The mixture was degassed with nitrogen for 1 h. The mixture was irradiated in an immersion apparatus with a 125 W high-pressure mercury arc for 18 h. The mixture was then washed with 20% sodium thiosulfate in water to oxidize traces of iodine and then with brine, dried with Na_2SO_4 and the solvents evaporated under vacuum to afford a crude mixture that was purified by chromatography over silica gel (eluent: 9:1 petroleum ether/ethyl acetate) to give 655 mg (2.9 mmol, 89%) of **12** together with 100 mg of unreacted ethyl 2-iodothiazole-5-carboxylate.

12: Oil. ^{1}H NMR (500 MHz, $CDCl_3$): δ = 1.36 (t, J = 7.1 Hz, 3 H, CH_3), 4.25 (q, J = 7 Hz, 2 H, CH_2), 6.45 (dd, J_1 = 3.5, J_2 = 1.5 Hz, 1 H, furyl 4-H), 7.35 (dd, J_1 = 3.5, J_2 = 0.5 Hz, 1 H, furyl 3-H), 7.50 (dd, J_1 = 1.5, J_2 = 0.5 Hz, 1 H, furyl 5-H), 9.21 (s,1 H, 5-H) ppm. ^{13}C NMR and DEPT (125 MHz, $CDCl_3$): δ = 14.4 (CH_3), 61.6 (CH_2), 111.7 (CH), 113.3 (CH), 128.4 (C), 144.1 (CH), 148.6 (C), 156.1 (CH), 157.5 (C), 161.9 (C) ppm. UV (CH_3CN): λ_{max} = 278 nm, ε = 7000 $dm^3 mol^{-1} cm^{-1}$. MS: *m*/*z* (%) = 223 (100) $[M]^+$, 178 (57.2), 166 (30.5), 151 (21.5), 138 (4.6), 122 (7.9), 111 (3.4), 99 (2.5), 85 (5.4), 57 (7.5), 45 (4.3), 29 (4), 18 (0.2). $C_{10}H_9NO_3S$ (223.25): calcd. C 53.80, H 4.06, N 6.27, S 14.36; found C 53.67, H 4.12, N 6.32, S 14.28.

Ethyl 3-(2-Thienyl)isothiazole-4-carboxylate (13): Compound **9** (74 mg, 0.26 mmol) was added to thiophene (3 g) in acetonitrile (80 mL). The mixture was degassed with nitrogen for 1 h. The mix-

ture was irradiated in an immersion apparatus with a 125 W high-pressure mercury arc for 13.5 h. The mixture was then washed with 20% sodium thiosulfate in water to oxidize traces of iodine and then with brine, dried with Na_2SO_4 and the solvents evaporated under vacuum to afford a crude mixture that was purified by chromatography over silica gel (eluent: 95:5 to 9:1 petroleum ether/ethyl acetate) to give 62 mg (0.25 mmol, 96%) of **13** together with 4 mg of ethyl thiazole-5-carboxylate.

13: Oil ^{1}H NMR (500 MHz, $CDCl_3$): δ = 1.38 (t, J = 7 Hz, 3 H, CH_3), 4.37 (q, J = 7 Hz, 2 H, CH_2), 7.10 (dd, J_1 = 5, J_2 = 4 Hz, 1 H, thienyl 4-H), 7.43 (dd, J_1 = 5, J_2 = 1 Hz, 1 H, thienyl 5-H), 7.93 (dd, J_1 = 4, J_2 = 1 Hz, 1 H, thienyl 3-H), 9.31 (s, 1 H, 5-H) ppm. ^{13}C NMR and DEPT (125 MHz, $CDCl_3$): δ = 14.4 (CH_3), 61.6 (CH_2), 127.6 (CH), 128.4 (C), 128.5 (CH), 129.5 (CH), 137.2 (C), 156.6 (CH), 161.5 (C), 162.2 (C) ppm. UV (CH_3CN): λ_{max} = 285 nm, ε = 7500 $dm^3 mol^{-1} cm^{-1}$. MS: m/z (%) = 239 (100) $[M]^+$, 211 (31), 194 (68), 167 (35), 151 (22), 122 (15). $C_{10}H_9NO_2S_2$ (239.31): calcd. C 50.19, H 3.79, N 5.85, S 26.80; found C 50.27, H 3.70, N 5.91, S 26.92.

Ethyl Thiazole-5-carboxylate: Oil. ^{1}H NMR (500 MHz, $CDCl_3$): δ = 1.18 (t, J = 7 Hz, 3 H, CH_3), 4.36 (q, J = 7 Hz, 2 H, CH_2), 8.45 (s, 1 H, 4-H), 8.88 (s, 1 H, 2-H) ppm. MS: m/z (%) =157 (20) $[M]^+$, 130 (21.4), 129 (66.75), 112 (100), 101 (8), 85 (9), 84 (22.7), 58 (8), 57 (26.7), 45 (12), 29 (8), 15 (0.7).

Ethyl 3-(5-Bromo-2-thienyl)isothiazole-4-carboxylate (14): Compound **9** (170 mg, 0.6 mmol) was added to 2-bromothiophene (1.5 g) in acetonitrile (80 mL). The mixture was degassed with nitrogen for 1 h. The mixture was irradiated in an immersion apparatus with a 125 W high-pressure mercury arc for 34 h. The mixture was then washed with 20% sodium thiosulfate in water to oxidize traces of iodine and then with brine, dried with Na_2SO_4 and the solvents evaporated under vacuum to afford a crude mixture that was purified by chromatography over silica gel (eluent: 95:5 to 9:1 petroleum ether/ethyl acetate) to give 66 mg (0.21 mmol, 35%) of **14** as an oil.

^{1}H NMR (500 MHz, $CDCl_3$): δ = 1.30 (t, J = 7 Hz, 3 H, CH_3), 4.37 (q, J = 7 Hz, 2 H, CH_2), 7.07 (d, J = 5 Hz, 1 H, thienyl 3-H), 7.42 (d, J = 5 Hz, 1 H, thienyl 4-H), 9.32 (s, 1 H, 5-H) ppm. ^{13}C NMR and DEPT (125 MHz, $CDCl_3$): δ = 14.4 (CH_3), 61.8 (CH_2), 127.6 (CH), 128.4 (C), 128.5 (CH), 132.3 (C), 137.2 (C), 156.7 (CH), 161.4 (C), 162.2 (C) ppm. MS: m/z (%) = 319 (0.8) $[M]^+$, 317 (0.8), 274 (3), 238 (51), 210 (100), 193 (14). $C_{10}H_8BrNO_2S_2$ (318.21): calcd. C 37.74, H 2.53, N 4.40, S 20.15; found C 37.63, H 2.60, N 4.35, S 20.07.

Ethyl 2-Phenylthiazole-5-carboxylate (15): Compound **9** (200 mg, 0.7 mmol), phenylboronic acid (110 mg, 0.9 mmol) and $[Pd_2(dba)_3]$ (32 mg, 0.035 mmol) were added to 1,2-dimethoxyethane (1.75 mL) in a conical vial and the resulting solution was degassed with a stream of nitrogen. Distilled water (0.1 mL) and 2 M K_2CO_3 in water (0.7 mL) were added and the mixture was stirred and heated at 100 °C for 6 h. The mixture was then diluted with ethyl acetate, dried with Na_2SO_4, passed through a short pad of Celite and the solvents evaporated under vacuum to give a crude product that was purified by chromatography over silica gel (eluent: 98:2 petroleum ether/ethyl acetate) to give 110 mg (0.47 mmol, 67%) of **15** as a white solid. M.p. 65–67.5 °C (lit.:[7] 64–65 °C).

^{1}H NMR (500 MHz, $CDCl_3$): δ = 1.41 (t, J = 7.5 Hz, 3 H, CH_3), 4.40 (q, J = 7.5 Hz, 2 H, CH_2), 7.52–7.46 (m, 3 H, phenyl, *p*- and *m*-H), 8.02–7.98 (m, 2 H, phenyl, *o*-H), 8.43 (s, 1 H, 4-H) ppm. ^{13}C NMR and DEPT (125 MHz, $CDCl_3$): δ = 14.5 (CH_3), 61.9 (CH_2), 127.1 (CH), 129.3 (CH), 129.3 (C), 131.4 (CH), 133.2 (C), 149.4 (CH), 161.7 (C), 173.5 (C) ppm. UV (CH_3CN): λ_{max} = 304 nm. MS: m/z (%) = 233 (100) $[M]^+$, 205 (48), 188 (50), 160 (42), 104 (20), 57 (43). $C_{12}H_{11}NO_2S$ (233.29): calcd. C 61.78, H 4.75, N 6.00, S 13.74; found C 61.69, H 4.84, N 6.09, S 13.70.

Photolysis of Ethyl 2-Phenylthiazole-5-carboxylate: Compound **15** (40 mg) was dissolved in acetonitrile (20 mL) in a Pyrex water jacket and irradiated with a 500 W high-pressure mercury arc. The reaction was monitored by GC–MS and stopped after 80 h (43% conversion). The solvent was then evaporated under vacuum to afford 45 mg of a crude mixture that was purified by semi-preparative TLC (1.0 mm layer, eluent: 9:1 petroleum ether/ethyl acetate) to give 9 mg of pure **11** (spectroscopic data identical to those reported).

Irradiation of *trans*-α,α′-Dimethylstilbene in the Presence of 11–14: A solution (50 mL) containing 2×10^{-4} M of **11**–**14** and 5×10^{-2} M *trans*-α,α′-dimethylstilbene[29] (**16**) in acetonitrile was irradiated in the presence of oxygen in a Pyrex tube surrounded by a Pyrex water jacket connected to a Haake F3 thermostat to maintain the temperature at 13.0 ± 0.1 °C in a Rayonet chamber with an 8 W lamp the output of which was centred at 350 nm. After 2 h, the solvent was removed under vacuum and the residual oil was analysed by ^{1}H NMR spectroscopy. Compound **17** showed peaks at δ = 2.42 (s, 1.5 H), 2.58 (s, 1.5 H), 5.97 (s, 0.5 H), and 6.18 (s, 0.5 H) ppm.

UV/Vis and Emission Spectroscopy: Solution electronic spectra in the region 230–400 nm were recorded at room temperature with a UV/Vis/NIR 05E Cary spectrophotometer by using 1.0 cm path length quartz cells. Absorption spectra were recorded at a scan rate of 200 nm/min at room temperature. Steady-state emission and excitation spectra were recorded with a HORIBA Jobin–Yvon FL3-11 Fluorolog-3 spectrometer at room temperature with a scan rate of 1 nm/s using solutions at concentrations 10^{-5}–10^{-6} M, giving rise to absorbance values less than 0.02 at the chosen excitation wavelengths. Excitation and emission spectra were corrected for source intensity (lamp and grating) and emission spectral response (detector and grating) by standard correction curves.

Photoluminescent quantum yields were measured by the method described by Demas and Crosby using anthracene (quantum yield: 0.27 in EtOH at room temperature) as the standard.[30]

Time-resolved measurements were performed with a HORIBA Jobin–Yvon IBH FL-322 Fluorolog-3 spectrometer using the time-correlated single-photon counting (TCSPC) option. NanoLED (375 nm; fwhm < 200 ps) with repetition rates between 10 kHz and 1 MHz was used to excite the sample. The excitation source was mounted directly on the sample chamber at 90° to a double-grating emission monochromator (2.1 nm/mm dispersion; 1200 grooves/mm) and collected with a TBX-4-X single-photon-counting detector. The photons collected at the detector are correlated by a time-to-amplitude converter (TAC) to the excitation pulse. Signals were collected by using an IBH Data Station Hub photon-counting module and data analysis was performed by using the commercially available DAS6 software (HORIBA Jobin Yvon IBH). The goodness of fit was assessed by minimizing the reduced χ^2 and visual inspection of the weighted residuals.

Computational Methods: Gaussian03 (revision D02) was used for the discussions of the computed geometries and UV/Vis spectra assignment.[31] The Turbomole 5.9 program was used to confirm the Gaussian03 UV/Vis assignments and to relax excited-state geometries for the emission peak wavelength computations.[32]

All the computations were based on density functional theory (DFT)[33] and time-dependent DFT (TD-DFT)[34] by using the B3LYP hybrid xc functional.[35] Geometry optimizations and TD-

DFT results from the Gaussian03 program were obtained at the B3LYP/6-31G(d,p) level of theory. For compounds **11** and **13**, the basis set accuracy was tested by using the 6-311G(2d,p) basis set. No significant changes in the description of the geometries and excited states were observed in comparison with the 6-31G(d,p) basis set.

Geometry optimizations were performed with default settings on geometry convergence (gradients and displacements), integration grid and electronic density (SCF) convergence. Redundant coordinates were used for the geometry optimization carried out with the Gaussian03 program. Analytical evaluation of the second-energy derivative matrix w. room temp. Cartesian coordinates (Hessian matrix) at the B3LYP/6-31G(d,p) level of theory confirmed the nature of the minima on the energy surface associated with the optimized structures.

Excited-state geometry optimizations were performed with the B3LYP xc functional and DZP basis set, as provided by the Turbomole 5.9 package. The Turbomole 5.9 default parameters were used for SCF, geometry optimization and integration grids. Geometries and UV/Vis spectra were computed to verify the Gaussian03 predictions.

Figures 1 and 3 were produced by using the Molekel 4.3 program.[36]

Supporting Information (see also the footnote on the first page of this article): GC–MS, ^{1}H and ^{13}C NMR, DEPT and computational details.

Acknowledgments

We thank the Italian Ministry of University and Research (MUR) (Project no. PRIN 2007) and the University of Basilicata for financial support.

[1] a) R. Antonioletti, M. D'Auria, A. De Mico, G. Piancatelli, A. Scettri, *Tetrahedron* **1985**, *41*, 3441–3446; b) R. Antonioletti, M. D'Auria, A. De Mico, G. Piancatelli, A. Scettri, *J. Chem. Soc. Perkin Trans. 1* **1985**, 1285–1288; c) M. D'Auria, R. Antonioletti, A. De Mico, G. Piancatelli, *Heterocycles* **1986**, *24*, 1575–1578; d) R. Antonioletti, M. D'Auria, F. D'Onofrio, G. Piancatelli, A. Scettri, *J. Chem. Soc. Perkin Trans. 1* **1986**, 1755–1758; e) M. D'Auria, A. De Mico, F. D'Onofrio, G. Piancatelli, *J. Chem. Soc. Perkin Trans. 1* **1987**, 1777–1780; f) M. D'Auria, A. De Mico, F. D'Onofrio, D. Mendola, G. Piancatelli, *J. Photochem. Photobiol. A: Chem.* **1989**, *47*, 191–201; g) M. D'Auria, *Gazz. Chim. Ital.* **1994**, *124*, 195–197; h) M. D'Auria, in: *Targets in Heterocyclic Systems, Chemistry and Properties* (Eds.: O. A. Attanasi, D. Spinelli), Italian Society of Chemistry, Rome, **1997**, vol. 1, pp. 277–302; i) M. D'Auria, E. De Luca, G. Mauriello, R. Racioppi, G. Sleiter, *J. Chem. Soc. Perkin Trans. 1* **1997**, 2369–2373; j) M. D'Auria, E. De Luca, G. Mauriello, R. Racioppi, *J. Chem. Soc. Perkin Trans. 1* **1998**, 271–273.

[2] M. D′Auria, C. Distefano, F. D'Onofrio, G. Mauriello, R. Racioppi, *J. Chem. Soc. Perkin Trans. 1* **2000**, 3513–3518.

[3] M. A. Ciufolini, Y.-C. Shen, *Org. Lett.* **1999**, *1*, 1843–1846.

[4] a) M. D'Auria, A. De Mico, F. D'Onofrio, G. Piancatelli, *Gazz. Chim. Ital.* **1986**, *116*, 747–748; b) M. D'Auria, A. De Mico, F. D'Onofrio, G. Piancatelli, *Synth. Commun.* **1987**, *17*, 491–497; c) M. D'Auria, A. De Mico, F. D'Onofrio, G. Piancatelli, *J. Org. Chem.* **1987**, *52*, 5243–5247; d) M. D'Auria, F. D'Onofrio, *Gazz. Chim. Ital.* **1988**, *118*, 633–635; e) M. D'Auria, A. De Mico, F. D'Onofrio, G. Piancatelli, *Gazz. Chim. Ital.* **1989**, *119*, 201–202; f) M. D'Auria, A. Vantaggi, *Photochem. Photobiol.* **1991**, *53*, 181–184; g) M. D'Auria, D. Tofani, *Tetrahedron* **1992**, *48*, 9315–9322; h) M. Herrnreiter, J. Kagan, X. Chen, K. Y. Lau, M. D'Auria, A. Vantaggi, *Photochem. Photobiol.* **1993**, *58*, 49–52; i) M. D'Auria, *Tetrahedron Lett.* **1994**, *35*, 3151–3154; j) M. D'Auria, G. Mauriello, *Photochem. Photobiol.* **1994**, *60*, 542–545; k) M. D'Auria, *J. Photochem. Photobiol. A: Chem.* **1995**, *91*, 187–192; l) M. D'Auria, E. De Luca, G. Mauriello, R. Racioppi, *Synth. Commun.* **1999**, *29*, 35–42.

[5] L. R. Beard, F. D. Colon, T. K. Song, P. J. A. Davies, D. M. Kochhar, R. A. S. Chandraratna, *J. Med. Chem.* **1996**, *39*, 3556–3563.

[6] M. Fong, W. J. Janowski, R. H. Prager, M. R. Taylor, *Aust. J. Chem.* **2004**, *57*, 599–604.

[7] M. Muraoka, T. Yamamoto, K. Enomoto, T. Takeshima, *J. Chem. Soc. Perkin Trans. 1* **1989**, 1241–1252.

[8] R. M. Paton, F. M. Robertson, J. F. Ross, J. Crosby, *J. Chem. Soc. Perkin Trans. 1* **1985**, 1517–1521.

[9] R. E. Wasylishen, H. M. Hutton, *Can. J. Chem.* **1977**, *55*, 619–624.

[10] V. J. Majo, J. Prabhakaran, J. J. Mann, J. S. Dileep Kumar, *Tetrahedron Lett.* **2003**, *44*, 8535–8537.

[11] J. P. Catteau, A. Lablache-Combier, A. Pollet, *J. Chem. Soc. C* **1969**, 1018.

[12] J. W. Pavlik, C. R. Pandit, C. J. Samuel, A. C. Day, *J. Org. Chem.* **1993**, *58*, 3407–3410.

[13] G. Vernin, J.-C. Poite, J. Metzger, J.-P. Aune, H. J. M. Dou, *Bull. Soc. Chim. Fr.* **1971**, 1103–1104.

[14] a) G. Vernin, R. Jauffred, C. Ricard, H. J. M. Dou, J. Metzger, *J. Chem. Soc. Perkin Trans. 2* **1972**, 1145–1150; b) C. Riou, G. Vernin, H. J. M. Dou, J. Metzger, *Bull. Soc. Chim. Fr.* **1972**, 2673–2678; c) J. W. Pavlik, P. Tongcharoensirikul, N. P. Bird, A. C. Day, J. A. Barltrop, *J. Am. Chem. Soc.* **1994**, *116*, 2292–2300.

[15] C. Vernin, C. Riou, H. J. M. Dou, L. Bouscasse, J. Metzger, G. Loridan, *Bull. Soc. Chim. Fr.* **1973**, 1743–1751.

[16] C. Riou, J. C. Poite, G. Vernin, J. Metzger, *Tetrahedron* **1974**, *30*, 879–898.

[17] a) M. Kojima, M. Maeda, *J. Chem. Soc. C* **1970**, 386–387; b) M. Maeda, M. Kojima, *J. Chem. Soc. Perkin Trans. 1* **1978**, 685–692.

[18] I. Saito, T. Morii, Y. Okamura, S. Mori, K. Yamaguchi, T. Matsuura, *Tetrahedron Lett.* **1986**, *27*, 6385–6388.

[19] I. Saito, T. Morii, S. Mori, K. Yamaguchi, T. Matsuura, *Tetrahedron Lett.* **1988**, *29*, 3963–3966.

[20] a) M. D'Auria, in: *Targets in Heterocyclic Systems, Chemistry and Properties*, (Eds: O. A. Attanasi, D. Spinelli), Italian Society of Chemistry, Rome, **1999**, vol. 2, pp. 233–279; b) M. D'Auria, *Heterocyles* **1999**, *50*, 1115–1136; c) M. D'Auria, *J. Org. Chem.* **2000**, *65*, 2494–2498; d) M. D'Auria, *Adv. Heterocycl. Chem.* **2001**, *79*, 41–88; e) M. D'Auria, *J. Photochem. Photobiol. A: Chem.* **2002**, *149*, 31–37; f) M. D'Auria, *Tetrahedron* **2002**, *58*, 8037–8042; g) M. D'Auria, R. Racioppi, *Lett. Org. Chem.* **2004**, *1*, 12–19; h) S. Buscemi, M. D'Auria, A. Pace, I. Pibiri, N. Vivona, *Tetrahedron* **2004**, *60*, 3243–3249.

[21] a) M. La Deda, I. Aiello, A. Grisolia, M. Ghedini, M. Amati, F. Lelj, *Dalton Trans.* **2006**, 390–399; b) A. Crispini, I. Aiello, M. La Deda, I. De Franco, M. Amati, F. Lelj, M. Ghedini, *Dalton Trans.* **2006**, 5124–5134; c) M. Amati, S. Belviso, P. L. Cristinziano, C. Minichino, F. Lelj, *J. Phys. Chem. A* **2007**, *111*, 13403–13414; d) M. Ghedini, T. Pugliese, M. La Deda, N. Godbert, I. Aiello, M. Amati, S. Belviso, F. Lelj, G. Accorsi, F. Barigelletti, *Dalton Trans.* **2008**, 4303–4318; e) T. Pugliese, N. Godbert, I. Aiello, M. La Deda, M. Ghedini, M. Amati, S. Belviso, F. Lelj, *Dalton Trans.* **2008**, 6563–6572.

[22] N. J. Turro, *Modern Molecular Photophysics*, University Science Books, **1991**.

[23] C. F. Foote, *Photochem. Photobiol.* **1991**, *54*, 659.

[24] K. Gollnick, A. Schnatterer, *Photochem. Photobiol.* **1986**, *43*, 365–378.

[25] a) K. Gollnick, S. Held, *J. Photochem. Photobiol. B: Biology* **1990**, *5*, 85–93; b) W. Adam, M. Bran, A. Griesbeck, V. Lucchini, E. Stabb, B. Will, *J. Am. Chem. Soc.* **1989**, *111*, 203–212.
[26] a) R. Akaba, K. Ohshima, Y. Kawai, Y. Obuchi, A. Negishi, H. Sakuragi, K. Tokumaru, *Tetrahedron Lett.* **1991**, *32*, 109–112; b) M. D'Auria, F. D'Onofrio, J. Suwinski, K. Swierczek, *Tetrahedron* **1993**, *49*, 3899–3906.
[27] K. Gollnick, S. Held, *J. Photochem. Photobiol. A: Chem.* **1993**, *70*, 135–145.
[28] R. S. Becker, J. Seixas de Melo, A. Maçanita, F. Elisei, *J. Phys. Chem.* **1996**, *100*, 18683.
[29] D. Lenoir, *Synthesis* **1977**, 553–554.
[30] J. N. Demas, G. A. Crosby, *J. Phys. Chem.* **1971**, *75*, 991–1024.
[31] M. J. Frisch, G. W. Trucks, H. B. Schlegel, G. E. Scuseria, M. A. Robb, J. R. Cheeseman, J. A. Montgomery Jr., T. Vreven, K. N. Kudin, J. C. Burant, J. M. Millam, S. S. Iyengar, J. Tomasi, V. Barone, B. Mennucci, M. Cossi, G. Scalmani, N. Rega, G. A. Petersson, H. Nakatsuji, M. Hada, M.Ehara, K. Toyota, R. Fukuda, J. Hasegawa, M. Ishida, T. Nakajima, Y. Honda, O. Kitao, H. Nakai, M. Klene, X. Li, J. E. Knox, H. P. Hratchian, J. B. Cross, V. Bakken, C. Adamo, J. Jaramillo, R. Gomperts, R. E. Stratmann, O. Yazyev, A. J. Austin, R. Cammi, C. Pomelli, J. W. Ochterski, P. Y. Ayala, K. Morokuma, G. A. Voth, P. Salvador, J. J. Dannenberg, V. G. Zakrzewski, S. Dapprich, A. D. Daniels, M. C. Strain, O. Farkas, D. K. Malick, A. D. Rabuck, K. Raghavachari, J. B. Foresman, J. V. Ortiz, Q. Cui, A. G. Baboul, S. Clifford, J. Cioslowski, B. B. Stefanov, G. Liu, A. Liashenko, P. Piskorz, I. Komaromi, R. L. Martin, D. J. Fox, T. Keith, M. A. Al-Laham, C. Y. Peng, A. Nanayakkara, M. Challacombe, P. M. W. Gill, B. Johnson, W. Chen, M. W. Wong, C. Gonzalez, J. A. Pople, *Gaussian 03*, *Revision D.02*, Gaussian, Inc., Wallingford, CT, **2004**.
[32] R. Ahlrichs, M. Bär, M. Häser, H. Horn, C. Kölmel, *Chem. Phys. Lett.* **1989**, *162*, 165–169.
[33] R. G. Parr, W. Yang, *Density Functional Theory of Atoms and Molecules*, Oxford University Press, New York, and Clarendon Press, Oxford, **1989**.
[34] a) M. E. Casida, in: *Recent Advances in Density Functional Methods* (Ed.: D. P. Chong), World Scientific, Singapore, **1995**, vol. 1, pp. 155–192; b) M. E. Casida, C. Jamorski, K. C. Casida, D. R. Salahub, *J. Chem. Phys.* **1998**, *108*, 4439–4449.
[35] A. D. Becke, *J. Chem. Phys.* **1993**, *98*, 5648–5652.
[36] a) P. Fluckiger, H. P. Luthi, S. Portmann, J. Weber, *Molekel 4.3*, Swiss Center for Scientific Computing, Manno (Switzerland), **2000**–**2002**; b) S. Portmann, H. P. Luthi, *Chimia* **2000**, *54*, 766.

Received: January 23, 2010
Published Online: May 11, 2010

